

# New $^{32}\text{Cl}(p,\gamma)^{33}\text{Ar}$ reaction rate for astrophysical rp-process calculations

H. Schatz,<sup>1,2,3</sup> C. A. Bertulani<sup>\*</sup>,<sup>1</sup> B. A. Brown,<sup>1,2</sup> R. R. C. Clement<sup>†</sup>,<sup>1,2</sup> A. A. Sakharuk,<sup>1,3</sup> and B. M. Sherrill<sup>1,2,3</sup>

<sup>1</sup>*National Superconducting Cyclotron Laboratory, Michigan State University, East Lansing, MI 48824, USA*

<sup>2</sup>*Dept. of Physics and Astronomy, Michigan State University, East Lansing, MI 48824, USA*

<sup>3</sup>*Joint Institute for Nuclear Astrophysics, Michigan State University, East Lansing, MI 48824, USA*

The  $^{32}\text{Cl}(p,\gamma)^{33}\text{Ar}$  reaction rate is of potential importance in the rp-process powering type I X-ray bursts. Recently Clement et al. [1] presented new data on excitation energies for low lying proton unbound states in  $^{33}\text{Ar}$  obtained with a new method developed at the National Superconducting Cyclotron Laboratory. We use their data, together with a direct capture model and a USD shell model calculation to derive a new reaction rate for use in astrophysical model calculations. In particular, we take into account capture on the first excited state in  $^{32}\text{Cl}$ , and also present a realistic estimate of the remaining uncertainties. We find that the  $^{32}\text{Cl}(p,\gamma)^{33}\text{Ar}$  reaction rate is dominated entirely by capture on the first excited state in  $^{32}\text{Cl}$  over the whole temperature range relevant in X-ray bursts. In the temperature range from 0.2 to 1 GK the rate is up to a factor of 70 larger than the previously recommended rate based on shell model calculations only. The uncertainty is now reduced from up to a factor of 1000 to a factor of 3 at 0.3-0.7 GK and a factor of 6 at 1.5 GK.

## I. INTRODUCTION

Proton capture rates in the rapid proton capture process (rp-process) play a critical role in determining energy release and final isotopic abundances in X-ray bursts [2, 3, 4, 5, 6, 7]. Reliable rates are therefore important for quantitative interpretations of observations. For example, new highly accurate data on burst profile changes over periods of years as observed in GS 1826-24 [8] would provide unique constraints on X-ray burst models if the nuclear physics of the rp-process would be well enough understood. As demonstrated in a number of X-ray burst model calculations [9, 10, 11] this is clearly not the case.

One problem is the reliability of proton capture rates in the rp-process, especially in X-ray bursts where the reaction path runs close to the proton drip line. Far from stability, proton capture rates typically are governed by a few resonances and therefore statistical models are not applicable over the entire relevant temperature range of 0.2-2 GK [12]. On the other hand, shell model calculations in the sd- [13, 14] and fp-shells [15, 16, 17] predict the properties of individual states but the typical uncertainty in level energies is about 100 keV even for the calculations of level shifts from mirror states. This translates into uncertainties of 3 or more orders of magnitude in the reaction rates [1, 18]. Currently, we expect that the majority of the proton capture rates in the rp-process suffer from such uncertainties.

Clement et al. [1] recently developed a new experimental method using radioactive beams at the National Superconducting Cyclotron Laboratory at Michigan State University to accurately determine excitation energies of nuclei in the rp-process path. They presented new results for the excitation energies of states in  $^{33}\text{Ar}$  that determine the  $^{32}\text{Cl}(p,\gamma)^{33}\text{Ar}$  reaction rate. Based on the new experimental data we present here a reevaluation of the  $^{32}\text{Cl}(p,\gamma)^{33}\text{Ar}$  rate, which is part of the reaction flow through the  $^{30}\text{S}$  -  $^{34}\text{Ar}$  region, an important bottleneck in the rp-process in X-ray bursts possibly related to the observed double peaked structure of some X-ray burst profiles [7].

The  $^{32}\text{Cl}(p,\gamma)^{33}\text{Ar}$  reaction rate recommended in reaction rate compilations [19] and used in X-ray burst models so far was a ground state capture rate based on shell model calculations with some experimental information from the  $^{33}\text{Ar}$  mirror nucleus  $^{33}\text{P}$  [14]. We use the new experimental data on states in  $^{33}\text{Ar}$  together with shell model calculations and a direct capture model to derive a new dramatically improved rate for the  $^{32}\text{Cl}(p,\gamma)^{33}\text{Ar}$  reaction. This differs from the initial discussion in Clement et al. [1] as we also take into account the contribution from proton capture on the first excited state in  $^{32}\text{Cl}$  at 89.9 keV. This state is thermally populated in an astrophysical plasma and as we will show here actually dominates the proton capture rate on  $^{32}\text{Cl}$  for the important temperature range between 0.2 and 1.5 GK. We also implement slight improvements in the penetrability calculations, evaluate the remaining shell model uncertainties and present the reaction rate in a form usable by astrophysical reaction networks.

---

\* Current Affiliation: Dept. of Physics, University of Arizona, Tucson, AZ 85721, USA

† Current Affiliation: Lawrence Livermore National Laboratory, 7000 East Ave. Livermore, CA 94550, USA

TABLE I: Properties of resonant states. Listed are spin and parity  $J^\pi$ , excitation energy  $E_x$ , center of mass resonance energy  $E_r$ , proton single particle widths  $\Gamma_{\text{sp}}$  for angular momenta  $l$ , spectroscopic factors  $C^2S$ , proton-decay width  $\Gamma_p$ ,  $\gamma$ -decay width  $\Gamma_\gamma$  and the resonance strength  $\omega\gamma$ . The upper part is for ground state capture, the lower part for capture on the first excited state in  $^{32}\text{Cl}$ .

$J^\pi$	$E_x(\text{MeV})$	$E_r(\text{MeV})$	$\Gamma_{\text{sp}}$		$C^2S$		$\Gamma_p(\text{eV})$	$\Gamma_\gamma(\text{eV})$	$\omega\gamma(\text{eV})$
			$l=0$	$l=2$	$l=0$	$l=2$			
5/2 <sup>+</sup>	3.364	0.021 ± 0.009		8.00e-42	2.90e-02	2.32e-02	2.32e-43	1.77e-02	2.32e-43
7/2 <sup>+</sup>	3.456	0.113 ± 0.009		1.90e-13	3.00e-03	5.70e-16	1.94e-03	7.60e-16	7.60e-16
5/2 <sup>+</sup>	3.819	0.476 ± 0.008		2.10e-02	4.30e-02	9.03e-04	1.54e-02	6.88e-04	6.88e-04
1/2 <sup>+</sup>	4.190	0.847 ± 0.100	6.30e+02	1.01e+01	6.70e-02	3.40e-02	4.26e+01	1.54e-01	5.11e-02
3/2 <sup>+</sup>	4.730	1.387 ± 0.100	2.50e+04	6.30e+02	3.00e-03	3.90e-02	9.96e+01	8.48e-02	4.33e-03
7/2 <sup>+</sup>	3.456	0.023 ± 0.009		1.30e-39	4.64e-03	6.03e-42	1.94e-03	4.83e-42	4.83e-42
5/2 <sup>+</sup>	3.819	0.386 ± 0.008	1.35e-01	1.50e-03	2.40e-02	4.39e-01	3.90e-03	1.54e-02	1.78e-03
1/2 <sup>+</sup>	4.190	0.757 ± 0.100		3.50e+00	2.27e-03	7.94e-03	1.54e-01	5.73e-06	5.73e-06
3/2 <sup>+</sup>	4.730	1.297 ± 0.100	1.60e+04	3.80e+02	7.49e-02	3.77e-03	1.20e+03	8.48e-02	3.13e-02

## II. RESONANT CAPTURE

The resonant reaction rate for capture on a nucleus in an initial state  $i$ ,  $N_A \langle \sigma v \rangle_{\text{res } i}$  can for isolated narrow resonances be calculated as a sum over all relevant compound nucleus states  $j$  above the proton threshold [20]:

$$N_A \langle \sigma v \rangle_{\text{res } i} = 1.540 \times 10^{11} (\mu T_9)^{-3/2} \sum_j \omega\gamma_{ij} e^{-E_{ij}/(kT)} \text{ cm}^3 \text{ s}^{-1} \text{ mole}^{-1} \quad (1)$$

where the resonance energy in the center of mass system  $E_{ij} = E_j - Q - E_i$  is calculated from the excitation energies of the initial  $E_i$  and compound nucleus  $E_j$  state.  $k$  is the Boltzmann constant. We adopt an experimental ground state mass difference  $Q$  (reaction Q-value) of  $3.343 \pm 0.007$  MeV [21].  $T_9$  is the temperature in GK and  $\mu$  is the reduced mass of the entrance channel in amu. The resonance strengths  $\omega\gamma_{ij}$  are in MeV and can be calculated for proton capture as

$$\omega\gamma_{ij} = \frac{2J_j + 1}{2(2J_i + 1)} \frac{\Gamma_{\text{p } ij} \Gamma_{\gamma j}}{\Gamma_{\text{total } j}} \quad (2)$$

where  $J_i$  is the target spin, and  $J_j$ ,  $\Gamma_{\text{p } ij}$ ,  $\Gamma_{\gamma j}$ ,  $\Gamma_{\text{total } j}$  are spin, proton decay width,  $\gamma$ -decay width, and total width of the compound nucleus state  $j$ . The total width is given by  $\Gamma_{\text{total } j} = \Gamma_{\gamma j} + \sum_i \Gamma_{\text{p } ij}$ . The proton decay widths depend exponentially on the resonance energy and can be calculated from the proton spectroscopic factor  $C^2S_{ij}$  and the single particle proton width  $\Gamma_{\text{sp } ij}$  as  $\Gamma_{\text{p } ij} = C^2S_{ij} \Gamma_{\text{sp } ij}$ . Here we calculated spectroscopic factors with the USD shell model as in Herndl et al. [14]. The single particle proton widths for most states were calculated from an exact evaluation of the proton scattering cross section from a Woods-Saxon potential well. This method is more precise than the penetrability model used by Herndl et al. [14] and Clement et al. [1], but agrees with previous work within 20%. The  $\gamma$  widths  $\Gamma_\gamma$  were taken from Herndl et al. [14]. This is justified as new experimental level energies are only available for the lower lying resonances where  $\omega\gamma$  is largely independent of  $\Gamma_\gamma$  as  $\Gamma_\gamma \gg \Gamma_p$ , and because for those states the changes in the  $\gamma$ -widths are less than 20%. The resulting properties of the resonance states in  $^{33}\text{Ar}$  are listed in Tab. I.

## III. DIRECT CAPTURE

The contribution to the  $^{32}\text{Cl}(\text{p},\gamma)^{33}\text{Ar}$  rate from direct capture into bound states has been calculated with a potential model [22] using a Woods-Saxon nuclear potential (central+spin-orbit) and a Coulomb potential of a uniform charge distribution. The nuclear potential parameters were determined by matching the bound state energies. Spectroscopic factors were calculated with the USD shell model as in Herndl et al. [14].

The direct proton capture rate  $N_A \langle \sigma v \rangle_{\text{dc } i}$  on the target nucleus in state  $i$  is usually parametrized in terms of the astrophysical S-factor  $S(E_0)$  in MeV barn at the Gamow window energy  $E_0$  [23]:

$$N_A \langle \sigma v \rangle_{\text{dc } i} = 7.83 \times 10^9 \left( \frac{Z}{\mu T_9^2} \right)^{1/3} S_i(E_0) e^{-4.29(Z^2 \mu / T_9)^{1/3}} \text{ cm}^3 \text{ s}^{-1} \text{ mole}^{-1} \quad (3)$$

TABLE II: Spectroscopic factors  $C^2S$  and astrophysical S-factors  $S(E_0)$  for direct capture into bound states in  $^{33}\text{Ar}$ . Listed are results for capture on the  $^{32}\text{Cl}$  ground state as well as on the first excited state in  $^{32}\text{Cl}$  (denoted with an asterix).  $J^\pi$  are spin and parity of the  $^{33}\text{Ar}$  final state,  $n$  is the node number,  $l_0$  the single particle orbital momentum, and  $j_0$  the total single particle angular momentum. The table only includes the significant contributions to the total S-factor.

$E_x(\text{MeV})$	$J^\pi$	$(nl_0)_{j_0}$	$C^2S$	$S(E_0)(\text{MeVbarn})$	$C^2S^*$	$S(E_0)^*(\text{MeVbarn})$
0	$1/2^+$	$2s_{1/2}$	0.08	6.56e-3		
		$1d_{3/2}$	0.67	4.47e-3	1.13	4.45e-3
1.359	$3/2^+$	$2s_{1/2}$			0.006	6.61e-4
		$1d_{3/2}$	0.19	1.78e-3	0.12	6.80e-4
1.798	$5/2^+$	$2s_{1/2}$			0.002	3.21e-4
		$1d_{3/2}$	0.15	1.84e-3	0.62	4.72e-3
		$1d_{5/2}$			0.021	1.65e-4
2.439	$3/2^+$	$2s_{1/2}$	0.031	4.32e-3	0.024	1.99e-3
		$1d_{3/2}$	0.17	1.09e-3	0.13	5.01e-4
3.154	$3/2^+$	$2s_{1/2}$	0.068	1.02e-2		
		$1d_{3/2}$	0.52	2.21e-3	0.17	4.35e-4
total				3.25e-2		1.39e-2

with  $Z$  being the charge number of the target nucleus.  $S_i(E_0)$  is the sum of the individual S-factors of the transitions from the initial state  $i$  into all bound states in the final nucleus. Table II lists the individual S-factors found for transitions into the 5 bound states of  $^{33}\text{Ar}$  from both, the  $^{32}\text{Cl}$  ground state and the first excited state as well as the total S-factor. For ground state capture, our total S-factor agrees within 30% with the one derived by Herndl et al. [14] using the same spectroscopic factors.

#### IV. NEW REACTION RATE

The relative population of the target nucleus states in thermodynamic equilibrium is simply given by the Saha equation. The total reaction rate is then the sum of the capture rate on all thermally excited states in the target nucleus weighted with their individual population factors:

$$N_A \langle \sigma v \rangle = \sum_i (N_A \langle \sigma v \rangle_{\text{res } i} + N_A \langle \sigma v \rangle_{\text{dc } i}) \frac{(2J_i + 1)e^{-E_i/kT}}{\sum_n (2J_n + 1)e^{-E_n/kT}}. \quad (4)$$

To obtain the total resonant reaction rate on a thermally excited target one can combine Eqs. 1, 2, and 4 and finds [25]:

$$N_A \langle \sigma v \rangle = \sum_j N_A \langle \sigma v \rangle_{0j} \frac{1}{G(T)} \left( 1 + \sum_{i>0}^{E_{ij}>0} \frac{\Gamma_{p ij}}{\Gamma_{p 0j}} \right) \quad (5)$$

where  $j$  sums over all resonances in the compound nucleus.  $i$  sums over the thermally populated states in the target nucleus as long as the resonance energy  $E_{ij} > 0$  with  $i = 0$  being the ground state.  $N_A \langle \sigma v \rangle_{0j}$  is the reaction rate contribution from ground state capture via the resonance  $j$ .  $G(T)$  is the temperature  $T$  dependent partition function of the target nucleus:

$$G(T) = (2J_0 + 1)^{-1} \sum_i (2J_i + 1) \exp(-E_i/kT) \quad (6)$$

This is similar to Eq. 10 in Fowler, Caughlan and Zimmerman [24]. Eq. 5 shows that for a given resonance the relative contribution from capture on each excited target state depends only weakly on temperature and the actual population of the excited state through the partition function  $G(T)$ . The contribution of excited states is mostly determined by the ratio of the proton widths to the excited state and to the ground state. Of course the temperature determines through  $\langle \sigma v \rangle_{0j}$  the relative importance of the various resonances.

In this work we consider only capture on the ground state and the first excited state in  $^{32}\text{Cl}$ . The  $^{32}\text{Cl}$  ground state is experimentally known to have spin and parity  $1^+$ . The spin for the experimentally known first excited state at 89.9 keV has not been determined unambiguously but we assign a spin of  $2^+$  based on the level structure of the

$^{32}\text{P}$  mirror and our shell model calculations. Excited states in the target will only play a role when for the relevant temperatures the thermal excitation timescale is smaller than the proton capture timescale. We can estimate the thermal excitation timescale for a  $\gamma$  induced transition from the ground state to the first excited  $2^+$  state in  $^{32}\text{Cl}$  by using the formalism of Ward and Fowler [26]. We assume a level lifetime of 280 ps from the mirror level in  $^{32}\text{P}$ , which is an upper limit as the mirror state is 12 keV lower in excitation energy. We find that even for the lowest relevant temperatures of 0.2 GK the excitation timescale is of the order of 30 ns. Assuming typical X-ray burst conditions with a density of  $10^6 \text{ g/cm}^3$  and a proton mass fraction of 0.7 the timescale for thermal excitation is always less than 0.2% of the proton capture timescale for all temperatures between 0.2 GK and 2 GK. Therefore, the first excited  $2^+$  state in  $^{32}\text{Cl}$  is always in thermal equilibrium with the ground state and Eq. 5 applies.

What is the role of higher lying excited states in  $^{32}\text{Cl}$ ? The second excited state in  $^{32}\text{Cl}$  is located at an energy of 466.1 keV. At such a high excitation energy the proton decay width  $\Gamma_p$  in Eq. 5 is already drastically reduced for the low lying resonances that have a significant ground state capture rate  $\langle \sigma v \rangle_{0j}$ . Therefore, the capture rate on the second excited state in  $^{32}\text{Cl}$  is negligible as either  $\Gamma_{p2j}$  or  $\langle \sigma v \rangle_{0j}$  in Eq. 5 are small for all resonances. Similar arguments apply to higher lying states.

The contributions from individual resonances and direct capture to the total  $^{32}\text{Cl}(p,\gamma)^{33}\text{Ar}$  reaction rate are shown in Fig. 1. The temperature dependent relative population of the ground and first excited state in  $^{32}\text{Cl}$  has been taken into account. Direct capture on the ground or the excited state is negligible over the entire relevant temperature range of 0.2-2 GK.

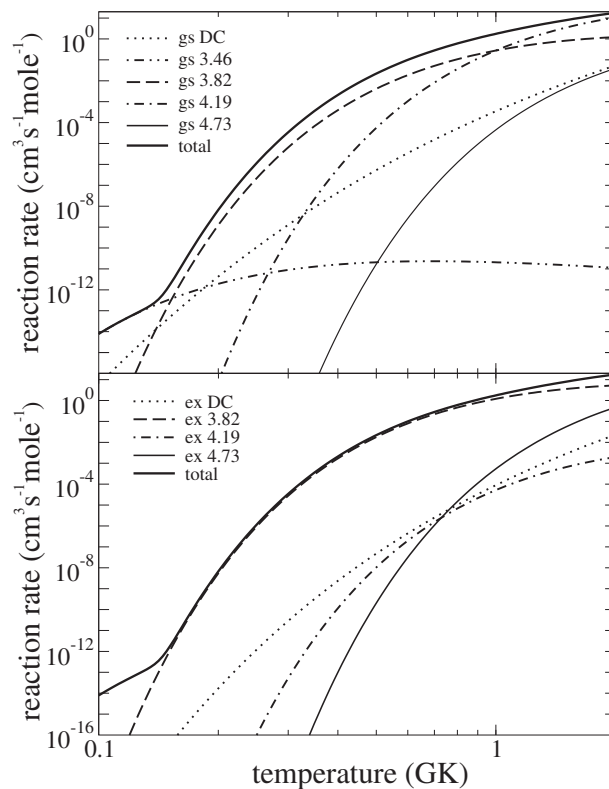


FIG. 1: The contributions of various individual resonances and through direct capture (DC) to the  $^{32}\text{Cl}(p,\gamma)^{33}\text{Ar}$  reaction rate as functions of temperature. In the legend, resonances are labeled with their excitation energy in  $^{33}\text{Ar}$ . The upper panel shows contributions from ground state capture, the lower panel contributions from capture on the first excited state in  $^{32}\text{Cl}$  in each case weighted with the relative population of the respective target state. In addition, both panels show the same total  $^{32}\text{Cl}(p,\gamma)^{33}\text{Ar}$  reaction rate for comparison. Contributions from ground state capture via the 3.36 MeV resonance and from capture on the first excited state via the 3.46 MeV resonance are too small to appear in this graph.

As Fig. 1 shows, the capture rate contributions from ground and excited target states vary greatly as  $\Gamma_p$  depends strongly on proton energy, spin, and nuclear structure. For  $^{32}\text{Cl}(p,\gamma)^{33}\text{Ar}$  the most dramatic change occurs for the  $5/2^+$  3.819 MeV resonance. For this resonance the spin of the excited state ( $2^+$ ) is one unit larger than for the ground state ( $1^+$ ) allowing for s-wave protons to populate the  $5/2^+$  resonance in addition to d-wave protons. As a result the proton width for capture on the excited state is a factor of 4.3 larger than for ground state capture despite the slightly lower proton energy. As a consequence (see Eq. 5) the resonant capture on the first excited state in  $^{32}\text{Cl}$  via the 3.819

TABLE III: Spectroscopic factors  $C^2S$  for  $d_{5/2}$  neutron removal from  $^{34}\text{Ar}$  to various  $5/2^+$  states in  $^{33}\text{Ar}$  calculated with the shell model effective interactions USD and USD05 and compared to experimental data [28] from the  $^{34}\text{S}$  to  $^{33}\text{P}$  mirror reaction for  $d_{5/2}$  protons. The excitation energies  $E_x$  of the  $5/2^+$  states are the experimentally known ones in the  $^{33}\text{P}$  mirror.

$E_x$ (MeV)	$C^2S$	$C^2S$	$C^2S$
Exp	Exp	USD05	USD
1.85	1.09	0.99	1.09
3.49	0.31	0.27	0.70
4.05	1.28	1.62	1.30
5.05	1.66	1.51	1.33

MeV  $5/2^+$  state in  $^{33}\text{Ar}$  becomes the dominant contribution to the stellar  $^{32}\text{Cl}(p,\gamma)^{33}\text{Ar}$  reaction rate for all relevant temperatures between 0.15 and 2 GK (see Fig. 1). This is despite the fact that the population of the first excited state in  $^{32}\text{Cl}$  for example at 0.3 GK is only 5%. As Eq. 5 demonstrates, the relative importance of contributions from capture on various states in the target is largely independent of their population (with the exception of their contribution to the partition function), what matters most is the proton width for the transition into the resonant state.

The remaining uncertainty from resonance energies ranges from 20 - 50% for the most important temperatures between 0.3 and 0.8 GK and increases to about a factor of 2 at 1.5 GK. It originates mainly from the small experimental uncertainties in the  $^{33}\text{Ar}$  excitation energies and the reaction Q-value. For the experimentally unknown higher lying levels we assume an uncertainty in the excitation energy of 100 keV, which is a typical deviation for shell model predictions of Coulomb shifts in this region. These levels only begin to contribute to the total reaction rate beyond around 1 GK and lead to the somewhat increased error at highest temperatures. At this level of error, other uncertainties in the shell model calculations now become relevant as well. The Woods-Saxon well used for the proton scattering widths is adjusted so that the total density for protons filled up to the Fermi energy reproduces the rms charge radius of nearby stable nuclei. We estimate an uncertainty of 5% in the Woods-Saxon radius parameter which leads to a 15% uncertainty in the proton decay widths.

In principle one could estimate the uncertainty of the shell model spectroscopic factors by comparing calculated spectroscopic factors with experimental data. No experimental data are available for the here relevant proton spectroscopic factors in  $^{33}\text{Ar}$  or the corresponding neutron spectroscopic factors in the  $^{33}\text{P}$  mirror. In addition, small spectroscopic factors are in general difficult to reliably extract from direct reaction cross sections due to the possibility of multi-step routes. However, we can test our shell model descriptions for the relevant states in  $^{33}\text{Ar}$  by comparing their relatively large neutron spectroscopic factors for  $^{34}\text{Ar}$  to  $^{33}\text{Ar}$  neutron removal with experimental data for the mirror proton spectroscopic factors for  $^{34}\text{S}$  to  $^{33}\text{P}$  proton removal. We limit the discussion to the  $5/2^+$  states, as the  $^{32}\text{Ar}(p,\gamma)^{33}\text{Ar}$  is dominated by the resonant contribution from the third  $5/2^+$  state in  $^{33}\text{Ar}$ . The calculations and experimental data for the  $5/2^+$  states are summarized in Tab. III. The calculations are carried out with the original USD interaction as well as close to final version of a new sd-shell interaction USD05 [27] obtained from a least squares fit to about 600 levels in the sd-shell nuclei. The spectroscopic factors are all large numbers and in good agreement with the experimental data from the mirror reaction. When calculated levels can be matched to experimental levels with the present degree of accuracy (about 100 keV) the comparison in Tab. III shows that the largest calculated spectroscopic factors are accurate to about 20% and the moderately large spectroscopic factors (as for the second  $5/2^+$  state) are accurate to about a factor of two.

In addition, we can look at variations in spectroscopic factors calculated with different shell model effective interactions. The spectroscopic factors for the important  $^{32}\text{Cl}(2^+)$  to  $^{33}\text{P}(5/2^+)$   $l=0$  transitions are shown in Tab. IV for the old USD interaction as well as the new USD05 interaction. All of the spectroscopic factors are small since the  $s_{1/2}$  orbit is mostly filled in  $^{32}\text{Cl}$ . The  $l=0$  spectroscopic factor summed over all final  $5/2^+$  states is only 0.131 for USD05. The comparison of the two interactions in Table 2 shows that the largest of the spectroscopic factors (including the one to the third  $5/2^+$  state of interest) agree to about 20%. Spectroscopic factors calculated with other effective interactions such as SDPOTA [29] or CWH [30], which also do a reasonable job of reproducing the energy levels for nuclei in the upper sd-shell, show a similar behavior. In general a small spectroscopic factor in the presence of other states with much larger spectroscopic factors may be very uncertain (as observed for many of the states in Tab. IV). However, when the spectroscopic factor is large compared to those for nearby states it can be relatively accurate. Thus the estimated theoretical error for small spectroscopic factors must be treated on a case by case basis.

To summarize, the shell model can describe the neutron single particle strength of the here relevant states within 20% to a factor of 2. In addition, the important  $l=0$  proton spectroscopic factor for the third  $5/2^+$  state is relatively large compared to other states and the total  $l=0$  proton single particle strength, and its calculation should therefore

TABLE IV:  $l = 0$  spectroscopic factors for the  $5/2^+$  states in  $^{33}\text{Ar}$  for proton capture on the  $2^+$  state in  $^{32}\text{Cl}$ . Spectroscopic factors  $C^2S$  and excitation energies  $E_x$  calculated with the USD and the USD05 interaction are compared.

$E_x$ (MeV)	$E_x$ (MeV)	$C^2S$	$C^2S$
USD05	USD	USD05	USD
1.99	2.00	0.0013	0.0006
3.42	3.83	0.0022	0.012
4.22	4.19	0.025	0.023
4.82	5.00	0.049	0.040
6.39	6.64	0.00002	0.0024
6.54	6.93	0.017	0.0024

TABLE V: Reaction rate  $N_A \langle \sigma v \rangle$  as a function of temperature  $T$ . Given is the recommended rate from this work (rec) as well as a lower and upper rate that reflect the estimated error bar.

$T$ (GK)	$N_A \langle \sigma v \rangle$ ( $\text{cm}^3/\text{s}/\text{mole}$ )		
	rec	lower	upper
0.1	7.85e-15	1.73e-15	2.81e-14
0.2	6.62e-09	3.20e-09	1.36e-08
0.3	3.44e-05	1.94e-05	6.04e-05
0.4	2.09e-03	1.27e-03	3.41e-03
0.5	2.21e-02	1.33e-02	3.67e-02
0.6	9.97e-02	5.80e-02	1.77e-01
0.7	2.82e-01	1.58e-01	5.37e-01
0.8	6.06e-01	3.27e-01	1.24e+00
0.9	1.09e+00	5.67e-01	2.39e+00
1.0	1.76e+00	8.75e-01	4.06e+00
1.5	7.94e+00	3.40e+00	2.03e+01
2.0	1.78e+01	7.48e+00	4.39e+01

be relatively reliable. We therefore estimate a factor of 2 uncertainty in the shell model spectroscopic factor in this specific case. To take into account other uncertainties such as the proton single particle widths discussed above, we adopt a total uncertainty of a factor of 2.5 for the  $^{32}\text{Cl}(p,\gamma)^{33}\text{Ar}$  reaction rate on top of the uncertainty from the resonance energies, which is accurately calculated as a function of temperature. The new reaction rate with its uncertainties is tabulated in Tab. V and displayed in Fig. 2. The total estimated uncertainty of the rate is about a factor of 3 at temperatures around 0.3-0.7 GK to about a factor of 6 at temperatures around 1.5 GK.

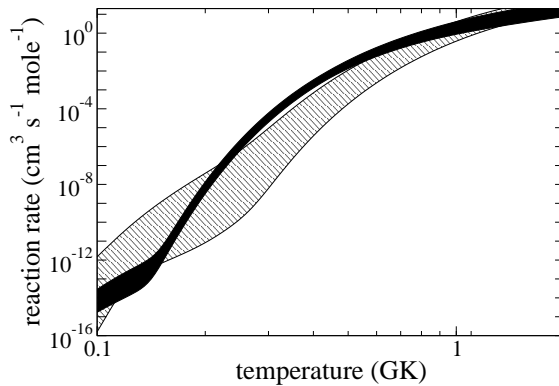


FIG. 2: Total  $^{32}\text{Cl}(p,\gamma)^{33}\text{Ar}$  reaction rate from this work (solid area) and previous shell model rate without experimental data (hatched area). The width of the area reflects the estimated uncertainty.

TABLE VI: Fit coefficients (see Eq. 7) for the recommended rate from this work (rec) as well as for the lower and upper limits that reflect the estimated error bar.

	$a_0$	$a_1$	$a_2$	$a_3$	$a_4$	$a_5$	$a_6$	$a_7$
rec	0.150730E+01	-0.539842E+01	-0.153745E+02	0.187918E+02	0.126139E+01	-0.208373E+00	-0.134957E+02	
	0.542869E+02	-0.782163E+01	0.367513E+03	-0.425108E+03	0.502875E+01	0.823457E+00	0.262097E+03	
lower	0.551123E+03	-0.158099E+02	0.886227E+03	-0.150891E+04	0.878013E+02	-0.495734E+01	0.714263E+03	
	-0.517996E+02	-0.156901E+01	-0.173733E+03	0.237842E+03	-0.114259E+02	0.538535E+00	-0.124462E+03	
upper	0.299493E+03	-0.143477E+02	0.705984E+03	-0.104556E+04	0.530983E+02	-0.269508E+01	0.533394E+03	
	-0.269317E+03	-0.794584E+00	-0.279531E+03	0.597651E+03	-0.505961E+02	0.399204E+01	-0.244496E+03	

Often, reaction rates are implemented into reaction network codes using a fit of the form:

$$N_A \langle \sigma v \rangle = \sum_i \exp(a_{0i} + a_{1i}T_9^{-1} + a_{2i}T_9^{-1/3} + a_{3i}T_9^{1/3} + a_{4i}T_9 + a_{5i}T_9^{5/3} + a_{6i}\ln T_9) \quad (7)$$

which is for example used in the `reaclib` reaction rate library. In Tab. VI we give fit parameters  $a_{ni}$  for our new recommended  $^{32}\text{Cl}(p,\gamma)^{33}\text{Ar}$  rate as well as for the upper and lower uncertainties. The fits are accurate to 5% and are valid between 0.1 and 10 GK. Beyond 2 GK we use the Hauser-Feshbach predictions from NON-SMOKER [32] using the procedure described by the NACRE collaboration [31]. The low temperature behavior is reasonable, so the fits can be used in model simulations that encounter lower temperatures.

## V. DISCUSSION

Our ground state capture rate for  $^{32}\text{Cl}(p,\gamma)^{33}\text{Ar}$  is similar to the rate given by Clement et al. [1]. Small differences arise from the slightly improved calculation of the proton single particle widths, the comprehensive reevaluation of the shell model uncertainties, and the modifications in the proton widths by taking into account transitions into excited target states. The major change however comes from the consideration of the capture on the first excited state in  $^{32}\text{Cl}$ . In the critical temperature range around 0.2-0.4 GK where for typical X-ray burst conditions (densities of  $10^{5-6}$  g/cm<sup>3</sup> and hydrogen mass fractions of 0.1-0.7) the reaction rate becomes comparable to the burst timescales (10-100 s) our rate is a factor of more than 4 larger than the ground state capture rate shown in Clement et al. [1]. In the same temperature range our rate is up to a factor of 70 larger than the recommended shell model based rate in Herndl et al. [14] (see Fig. 3).

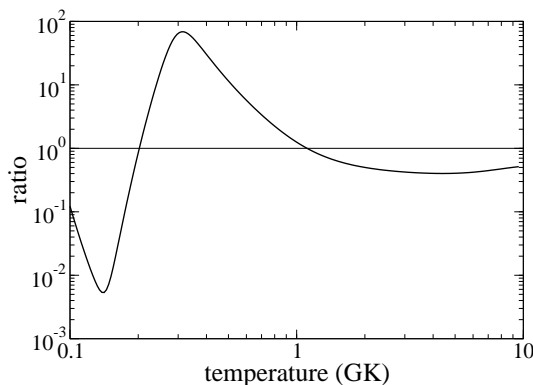


FIG. 3: Ratio of the  $^{32}\text{Cl}(p,\gamma)^{33}\text{Ar}$  reaction rate of this work to the rate calculated by Herndl et al. [14].

The impact of thermally excited states in the target nucleus on a reaction rate is often expressed in terms of a "Stellar Enhancement Factor", or SEF, which is defined as the ratio of the actual capture rate to the ground state capture rate. Fig. 4 shows the SEF determined in this work. The enhanced proton capture rate from the first excited state in  $^{32}\text{Cl}$  leads to a dramatic enhancement of the reaction rate of up to a factor of 5 at the important temperatures around 0.2-0.4 GK. Recent reaction rate compilations typically use SEFs that are calculated with the

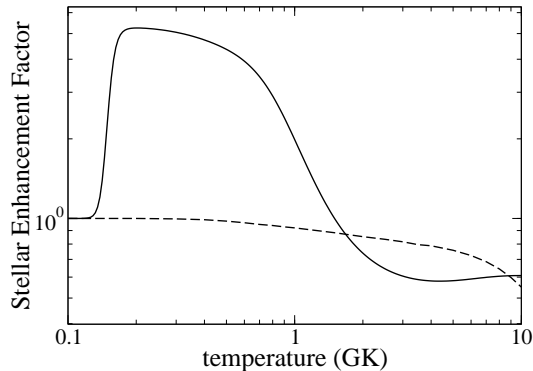


FIG. 4: Stellar enhancement factor derived in this work (solid line) and from the statistical model code NON-SMOKER (dashed line).

statistical Hauser-Feshbach model [19, 31]. For comparison we also show in Fig. 4 the SEF obtained with the Hauser-Feshbach code NON-SMOKER [32]. Clearly in this case a statistical approach to calculating the SEF does not give the correct result, even in the temperature range above 0.7 GK where strictly speaking the Hauser-Feshbach model is expected to be applicable [12, 32]. This is no surprise as here the SEF is entirely dominated by the properties of a single resonance. However, this example illustrates that large uncertainties can be introduced when using statistical model SEFs far from stability when reaction rates are dominated by a few resonances only. A better general approach would be to calculate SEFs within the shell model.

Clearly accurate masses and excitation energies are the single most important step for improving the accuracy of theoretical reaction rates. For comparison Fig. 2 also shows the uncertainty band of the reaction rate for the case that none of the excitation energies would be known experimentally, a situation that is very common along the rp-process path. Clearly, without experimental excitation energies reaction rates in the rp-process far from stability can be uncertain by many orders of magnitude. A measurement of excitation energies and Q-values to better than 10 keV can reduce this uncertainty to about a factor of 3.

To obtain in critical cases even more precise reaction rates one would need to perform indirect measurements of spectroscopic factors, or perform a direct measurement of the reaction rate at astrophysical energies. Note, however, that in this particular case a direct measurement would not be possible as the reaction rate is dominated by capture on the first excited state in the  $^{32}\text{Cl}$  target nucleus. This underlines the importance of indirect methods in determining accurate stellar reaction rates.

We thank M. Wiescher for pointing out the importance of the timescale for thermal excitation and O. Sorlin for pointing out the potential relevance of the first excited state in  $^{32}\text{Cl}$ . This work was supported by NSF grants PHY 0110253 (NSCL) and PHY 0216783 (Joint Institute for Nuclear Astrophysics). H.S. acknowledges support through the Alfred P. Sloan Foundation. B.A.B. acknowledges support from NSF grant PHY-0244453. C.A.B. thanks for support by the U.S. Department of Energy under grant No. DE-FG02-04ER41338.

- 
- [1] R.R.C. Clement *et al.* Phys. Rev. Lett. **92**, 2502 (2004).
  - [2] R. K. Wallace and S. E. Woosley, Ap. J. Suppl. **45**, 389 (1981).
  - [3] H. Schatz *et al.*, Phys. Rep. **294**, 167 (1998).
  - [4] M. Wiescher and H. Schatz, Journ. Phys. G Topical Review **25**, R133 (1999).
  - [5] H. Schatz *et al.*, Nucl. Phys. A **654**, 924 (1999).
  - [6] F.-K. Thielemann *et al.*, Prog. in Part. and Nucl. Phys. **46**, 46 (2001).
  - [7] J. L. Fisker, F.-K. Thielemann, and M. Wiescher, Ap. J. Lett. **608L**, 61 (2004).
  - [8] D. K. Galloway *et al.*, Ap. J. **601**, 466 (2004).
  - [9] O. Koike *et al.* Astron. Astrophys. **342**, 464 (1999).
  - [10] B. A. Brown *et al.* Phys. Rev. C **65** (2002) 5802.
  - [11] S. E. Woosley *et al.* Ap. J. Suppl. **151**, 75 (2004).
  - [12] T. Rauscher, F.-K. Thielemann, and K.-L. Kratz, Phys. Rev. C **56**, 1613 (1997).
  - [13] B. A. Brown and B. H. Wildenthal, Ann. Rev. of Nucl. Part. Sci. **38**, 29 (1988).



- [14] H. Herndl *et al.* Phys. Rev. C **52**, 1078 (1995).
- [15] M. Honma, T. Otsuka, B. A. Brown and T. Mizusaki, Phys. Rev. C **65**, 061301 (2002).
- [16] M. Honma, T. Otsuka, B. A. Brown and T. Mizusaki, Phys. Rev. C **69**, 034335 (2004).
- [17] J. L. Fisker *et al.* At. Data. Nuc. Dat. Tables **79**, 241 (2001).
- [18] H. Schatz *et al.* Phys. Rev. Lett. **79**, 3845 (1997).
- [19] C. Iliadis *et al.* Ap. J. Suppl. **134**, 151 (2001).
- [20] W. A. Fowler and F. Hoyle, Ap. J. Suppl. **9**, 201 (1964).
- [21] G. Audi, A. H. Wapstra, and C. Thibault, Nucl. Phys. A **729**, 337 (2003).
- [22] C.A. Bertulani, Comput. Phys. Commun. **156**, 123 (2003).
- [23] W. A. Fowler, G. R. Caughlan, and B. A. Zimmerman, Annu. Rev. Astro. Astrophys. **5**, 525 (1967).
- [24] W. A. Fowler, G. R. Caughlan, and B. A. Zimmerman, Annu. Rev. Astro. Astrophys. **13**, 69 (1975).
- [25] G. Vanraeynest *et al.*, Phys. Rev. C **57**, 2711 (1998).
- [26] R. A. Ward and W. A. Fowler, Ap. J. **238**, 266 (1980).
- [27] B. A. Brown and W. A. Richter, in the proceedings of the International Symposium on Correlation Dynamics in Nuclei, Tokyo, Japan, January 31 to February 4, 2005; and private communication.
- [28] S. Kahn *et al.* Nucl. Phys. A **481**, 253 (1988).
- [29] B. A. Brown, W. A. Richter, R. E. Julies and B. H. Wildenthal, Ann. Phys. **182**, 191 (1988).
- [30] B.H. Wildenthal in “Elementary Modes of Excitation in Nuclei”, Proceedings of the International School of Physics “Enrico Fermi”, course 69, edited by A. Bohr and R.A. Broglia (North-Holland, 1977), p. 383; B.H. Wildenthal and W. Chung in ‘Mesons in Nuclei’, edited by M. Rho and D.H. Wilkinson, (North-Holland, 1979), p. 723.
- [31] C. Angulo *et al.* Nucl. Phys. A **656**, 3 (1999).
- [32] T. Rauscher and F.-K. Thielemann, At. Dat. and Nucl. Dat. Tables **75**, 1 (2000), obtained via <http://quasar.physik.unibas.ch/~tommy/nosmo.html>